UHECR2024
Self-induced confinement of UHECRs closeby their sources

Presenter: Alessandro Cermenati

Supervisors: Roberto Aloisio, Pasquale Blasi, Carmelo Evoli

Gran Sasso Science Institute (GSSI), L'Aquila (AQ), Italy
Istituto Nazionale di Fisica Nucleare (INFN), Laboratori Nazionali del Gran Sasso (LNGS), Assergi (AQ), Italy

Pierre Auger Observatory, Malargue 2024, November

Ultra High-Energy Cosmic Rays

Spectrum and composition beyond the "second knee" (Abreu *et al.* (2021); Aab *et al.* (2016)):

- spectral breaks most likely determined by the composition:
  - Ankle: $\approx$ end of the proton contribution;
  - Instep: Subsequent cutoff of different nuclear species;
- Predominantly mixed mass composition:
  - 100 PeV - 3 EeV: increasingly lighter with the energy;
  - $\gtrsim$ 3 EeV: increasingly heavier, compatible with Peter's cycle.

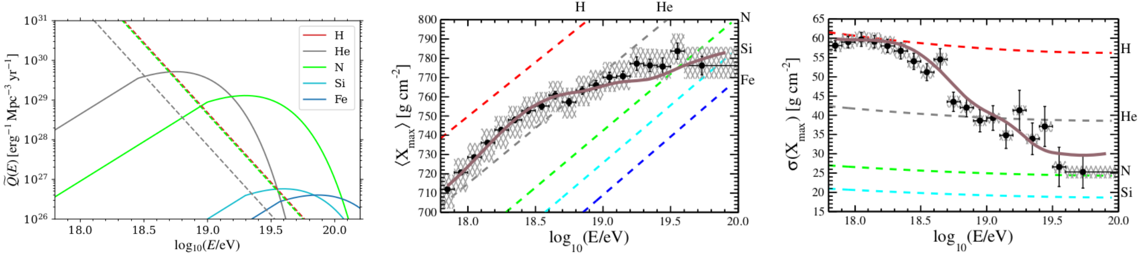

- Low-Energy population: soft injection, $\gamma \approx 3, 3.5$; mainly protons and light nuclei (Halim *et al.* (2023)).
- High-Energy population: hard injection, $\gamma \lesssim 1$ (also negative values); mainly nuclei
  - Transport effect: $\rightarrow$ Magnetic horizon: B $\approx 50 - 100$ nG (Halim *et al.* (2024)).
  - Acceleration mechanism: unipolar induction, stochastic acceleration in GRB, magnetic reconnections.

Interpretation of the "High-Energy" population

At energies above the *ankle* ($\approx 10^{18.5}$ eV):

- The spectral features are compatible with subsequent rigidity cutoff of different nuclear species.
- Maximum energy for protons below the ankle ($E_{max} \approx 2$ EeV).
- The X_{max} and $\sigma(X_{max})$ behaviors indicate a continuous increase of the mass composition.

In terms of sources' characterization, the population accelerating cosmic rays at Ultra-High Energies is required to:

- Accelerate nuclei $\rightarrow$ acceleration environment polluted by star-forming activity.
- Have a relatively low maximum rigidity, $R_{max} \approx 10^{18.2}$ V.
- Produce a negative spectral index, $\gamma \approx -2$.

The latter condition is better interpreted in terms of transport, instead of acceleration:

- Large magnetic field ($\approx 50 - 100$ nG) in between the Earth and the closest sources.
- Magnetic confinement within the source environment.

Can the excitation of the Non-Resonant Streaming Instability by UHE Cosmic Rays help to explain the magnetic confinement within, or closeby, the source environment?

Self-induced confinement: source and IGM model

Source		Environment (IGM)	
Luminosity (in CRs)	$L \approx 10^{45}$ erg/s	Magnetic field	$B_0 \approx 1$ nG
Radial Size	$R_s \approx 1$ Mpc	Correlation length	$\lambda_B \approx 10$ Mpc
Energy range	$E_{\rm min} \approx$ GeV, $E_{\rm max} \approx 3$ EeV	Gas density	$\rho_b \approx \delta 4 \cdot 10^{-31}$ g/cm^3
Lasting of the injection	$T_{\rm age} \approx 10$ Gyr	Temperature	$T \approx 10^4$ K

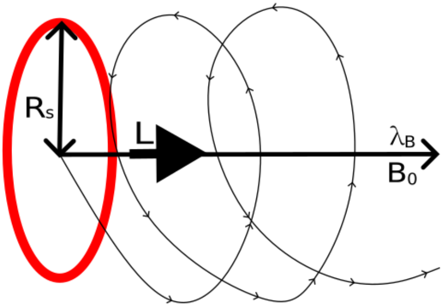

Following the same description as Blasi *et al.* (2015), we consider as "source" any object which accelerates UHECRs or embed an accelerator of UHECRs:

- Injection spectrum $q_s(E) \propto L \times E^{-2} \times f(E_{\rm cut})$.
- Characteristic energy-scale: $R_L(E) = R_s \to E \approx$ EeV.
- Particles with $R_L(E) \leq \lambda_B \to E_{\rm magn} \lesssim 10$ EeV follow the magnetic field lines.
- The current induced by UHECRs leaving the source is

$$J(>E) = e\frac{c}{2}\int_E^{E_{\rm magn}} dEn(E) \approx \frac{eEq(E)}{\pi(R_s + R_L(E))^2}$$

Non Resonant Streaming Instability

- The non-resonant branch of the streaming instability develops if the energy density carried by the UHECR current is larger than the magnetic energy density (Bell (2004)):

$$\frac{EJ(>E)}{ec} > \frac{B_0^2}{4\pi} \quad \Rightarrow \quad L \gtrsim 10^{42}\ \mathrm{erg/s}\, B_{\mathrm{nG}}^2 R_{\mathrm{Mpc}}^2$$

- Differently from the gyroresonant instability, magnetic perturbations are excited at wavelengths smaller than the Larmor radius of the particles, and have a faster growth rate:

$$k_{\max}(E) = \frac{4\pi}{cB_0} J(>E) >> 1/R_L(E) \quad \Longrightarrow \quad \gamma_{\max}(E) = V_A k_{\max}(E) = \frac{B_0}{\sqrt{4\pi\rho}} k_{\max}(E)$$

- In order to develop the instability, the Larmor radius of the thermal protons must be smaller than the growing wavelengths, $k_{\max} R_{L,th} \lesssim 1$ (Zweibel and Everett (2010)). This translates into a lower limit on the original magnetic field to develop the effect:

$$B_0 > \left(\frac{16 L^2 m_p k_B T_{\mathrm{IGM}}}{\Lambda^2 E_{\min}^2 R^4}\right)^{1/4} \approx 10^{-4}\ \mathrm{nG} \left(\frac{L}{10^{45}\ \mathrm{erg/s}}\right)^{1/2} \left(\frac{T_{\mathrm{IGM}}}{10^4\ \mathrm{K}}\right)^{1/4} \left(\frac{R}{\mathrm{Mpc}}\right)^{-1} \left(\frac{E_{\min}}{\mathrm{PeV}}\right)^{-1/2}.$$

Non Resonant Streaming Instability II

- Initially, the magnetic field perturbations grow on a scale k_{max}^{-1} up to values $\delta B/B_0 > 1$. The saturation is achieved through the Lorentz force $J \times B$, which stretches the perturbations on larger scales, matching the Larmor radius of the particles and strongly impacting the CR current:

$$\frac{\delta B_{sat}^2}{4\pi} \approx \frac{EJ(>E)}{ec} \quad \Longrightarrow \quad \delta B_{sat} \approx \sqrt{\frac{4L}{\Lambda c R_s^2}} \sim 25 \text{ nG} \left(\frac{L}{10^{45} \text{ erg/s}}\right)^{1/2} \left(\frac{R_s}{\text{Mpc}}\right)^{-1}$$

- On a timescale of a few (5-10) gyration periods (γ_{max}^{-1}), the excited turbulences can resonantly scatter and diffuse cosmic rays up to a critical energy scale E$_c$:

$$\tau_{sat}(E_c) = \frac{5}{\gamma_{max}(E_c)} = T_{age} \Rightarrow D(E) = \frac{c}{3} \frac{E_c}{e\delta B_{sat}} \left[\frac{E}{E_c} + \left(\frac{E}{E_c}\right)^2\right] \approx 4 \frac{\text{Mpc}^2}{\text{Gyr}} \left(\frac{L}{10^{45} \text{ erg/s}}\right)^{-\frac{1}{2}} \left(\frac{R}{\text{Mpc}}\right) \left(\frac{E}{\text{EeV}}\right)$$

- In addition, the isotropization of the CR density within the flux tube leads to a pressure gradient that acts on the plasma, setting it into motion at the Alfven speed (Blasi and Amato (2019))

$$V_A = \frac{\delta B_{sat}}{\sqrt{4\pi\rho}} \sim 0.1 \text{ Mpc/Gyr} \left(\frac{L}{10^{45} \text{erg/s}}\right)^{1/2} \left(\frac{R}{\text{Mpc}}\right)^{-1} \delta^{1/2}$$

Low energy suppression

A low-energy suppression of the escaping flux appears as a result of diffusion on the self-generated magnetic perturbations:

$$T_{\rm esc}^{-1}(E) = \frac{V_A}{\lambda_B} + \frac{D(E)}{\lambda_B^2} \qquad\qquad Q_{\rm scr}(E) \approx q_s(E) \times \mathcal{H}(T_{\rm age} - T_{\rm esc}(E))$$

$$T_{\rm esc}(E) = T_{\rm age} \quad \Rightarrow \quad E_{\rm cut} \approx 0.4\,{\rm EeV} \left(\frac{L}{10^{45}\,{\rm erg/s}}\right)^{1/2} \left(\frac{R}{\rm Mpc}\right)^{-1} \left(\frac{\lambda_{\rm B}}{10\,{\rm Mpc}}\right)^{2}$$

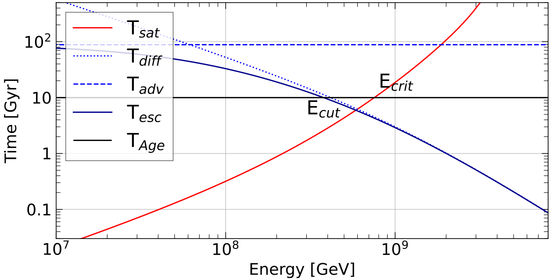

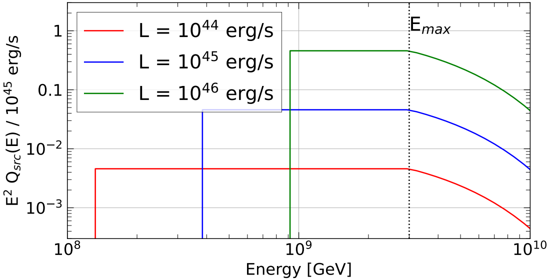

Emissivity of different sources

- Advection implies a maximum luminosity for the confinement to be effective: for too high current intensity L/R^2, the Alfvén speed becomes too high and particles are evacuated from the magnetized bubble: $T_{\rm age} < \lambda_B/V_A \Rightarrow L_{\rm max} \approx 10^{47}$ erg/s $\lambda^2_{\rm 10Mpc} R^2_{\rm Mpc}$.
- The low-energy suppression depends on the source's power, $D(E) \propto \frac{E_c(L)}{\delta B(L)}$.
- The overall emissivity computed for a population of sources distributed as a power-law, $\Phi(L) \propto L^{-\beta}$, results in an injection spectral index unrelated to the acceleration process $Q_{\rm src}(E) \propto E^{2(1-\beta)}$:
  - For steep distributions ($\beta > 2$) the suppression is dominated by the less powerful / most abundant sources.
  - For flatter distributions the suppression is dominated by the most powerful sources.

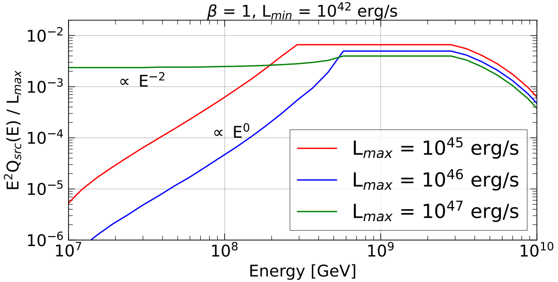

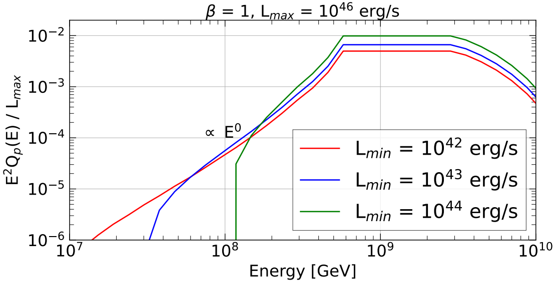

Self-induced confinement: particles emissivity

Cosmic Rays Emissivity: $Q_{(A,Z)}(E,z) \approx \int dL \cdot \Phi(L,z) \times q^{\rm acc}_{(A,Z)}(E) \times \mathcal{H}\left[E - E_{\rm cut}(L)\right]$
VHE neutrinos, produced through the photopion interaction, can be produced on the EBL:

- by protons confined within the magnetized cocoons:

$$Q_{\nu}^{\rm bubbles}(E_\nu, z) \approx \int dL \cdot \Phi(L,z) \times q_{\rm acc}(E_p) \times \tau_{\rm esc}(E_p) \times \mathcal{R}(E_\nu, E_p, n_\gamma(\epsilon)),$$

- by released protons that can reach the Earth (cosmogenic neutrinos):

$$Q_{\nu}^{\rm cosmo}(E_\nu, z) \propto n_p(E_p, z) \times \mathcal{R}(E_\nu, E_p, n_\gamma(\epsilon)),$$

  with $n_p(E_p, z)$ the equilibrium density of protons released into the Universe Berezinsky *et al.* (2006).

- We estimate the two neutrino contributions for reasonable assumptions on the source's population:
  - Various shapes of the $\Phi(L)$, resembling the luminosity distribution of AGN's / Galaxies.
  - Up to $z_{\rm max} = 3$, with no redshift evolution of the sources.
  - $\Phi(L)$ normalized to match the proton spectrum as observed by PAO (Abreu *et al.* (2021); Aab *et al.* (2016)).
  - Both confined and released protons interact with the CMB and the EBL (Saldana-Lopez *et al.* (2021)).
  - The contribution to the VHE neutrino flux comes mainly from confined protons in the PeV - 100 PeV energy range, depending on the power of the dominant sources.

Production of neutrinos

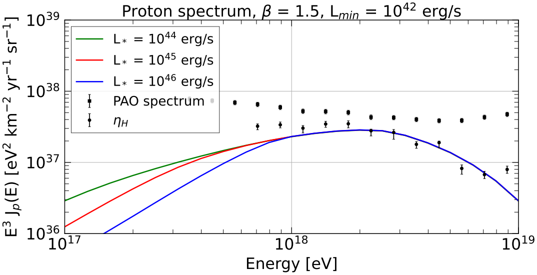

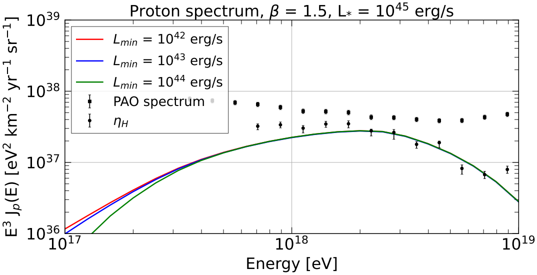

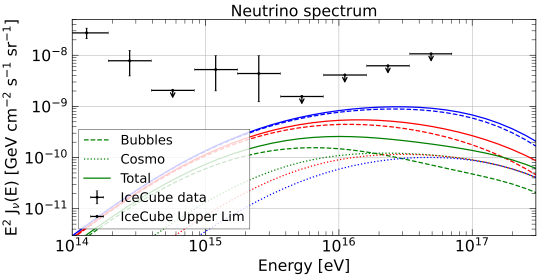

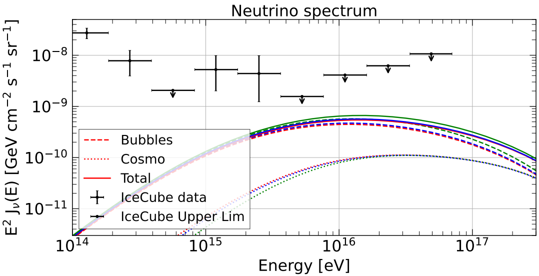

First results

- The excitation of the NRSI when the UHECR current leaves the source can help the interpretation of the UHECR spectrum and mass composition without invoking any exotic acceleration mechanism:
  - It naturally induces magnetic confinement close to the sources.
  - It needs an original magnetic field of order $B \approx 0.1 - 1$ nG $\lambda_{10\text{Mpc}}$.
    The turbulent amplified field only exists in the presence of UHECR sources.
  - The shape of the spectrum below the suppression is unrelated to the acceleration mechanism if different sources' luminosities are considered.
  - Confined protons produce more neutrinos than the released ones.
  - The cosmogenic neutrino flux does not overshoot the upper limits posed by Ice Cube (Aartsen *et al.* (2013)).
- To reach a suppression of the flux at the EeV energy scale, some requirements must be fulfilled:
  - The current intensity should be high enough to produce the NRSI, but not too high to evacuate the magnetized cocoons:

$$L_{\text{min}} \approx 10^{42}\ \text{erg/s}\, R_{\text{Mpc}}^2\, B_{\text{nG}} < L < L_{\text{max}} \approx 10^{47}\ \text{erg/s}\, \lambda_{10\text{Mpc}}^2 R_{\text{Mpc}}^2$$

  - A too-high original magnetic field will prevent the instability from developing, but if it's too low, the thermal plasma cannot respond to the perturbations:

$$B_{\text{low}} \approx 10^{-4}\text{nG}\, L_{45}^{1/2} R_{\text{Mpc}}^{-1} E_{\text{PeV}}^{-1/2} < B_0 < \delta B \approx 25\,\text{nG}\, L_{45}^{1/2} R_{\text{Mpc}}^{-1}$$

- The power and magnetic field requirements suggest Cosmic Filaments, fed by Galaxy Clusters, are the best candidates for the NRSI to impact the UHECRs transport in the Universe up to the EeV energy scale.

Next step: nuclei

Physical properties of UHECR sources and IGM determines shape, normalization and suppression of the released spectrum:

- Energetic argument: the emissivity needed to reproduce the observed UHECR energy density is:
  $\mathcal{L} \approx 10^{45}$ erg/yr/Mpc$^3 \approx n(> L) \times L$.
- Source density can be constrained from directional anisotropies Bister and Farrar (2024):
  $n(> L) \gtrsim 10^{-4}$ Mpc$^{-3} \Rightarrow L \approx 10^{41}$ erg/s. (The impact of the magnetic confinement must be included!)
- The low energy suppression depends on sources' power (L), and IGM properties (B_0, λ_B).

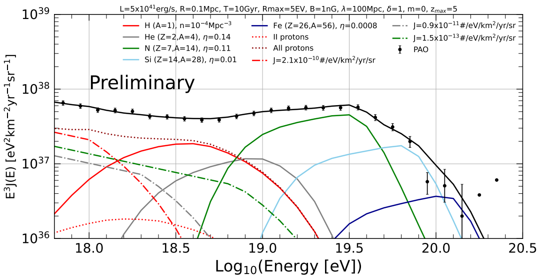

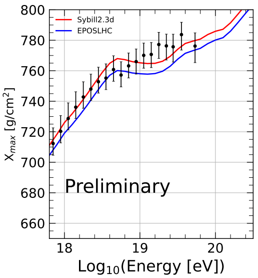

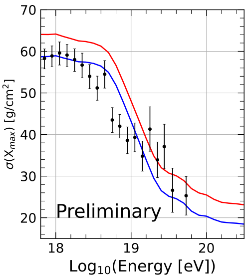

End of the presentation

P. Abreu, M. Aglietta, J. M. Albury et al., The European Physical Journal C **81**, 1 (2021).

A. Aab, P. Abreu, M. Aglietta et al., Physics Letters B **762**, 288 (2016).

A. A. Halim, P. Abreu, M. Aglietta et al., Journal of Cosmology and Astroparticle Physics **2023** (05), 024.

A. A. Halim, P. Abreu, M. Aglietta et al., Journal of Cosmology and Astroparticle Physics **2024** (07), 094.

P. Blasi, E. Amato and M. D'Angelo, Phys. Rev. Lett. **115**, 121101 (2015), arXiv:1508.02866 [astro-ph.HE] .

A. R. Bell, MNRAS **353**, 550 (2004).

E. G. Zweibel and J. E. Everett, The Astrophysical Journal **709**, 1412 (2010).

P. Blasi and E. Amato, Phys. Rev. Lett. **122**, 051101 (2019).

V. Berezinsky, A. Gazizov and S. Grigorieva, Phys. Rev. D **74**, 043005 (2006).

A. Saldana-Lopez, A. Domínguez, P. G. Pérez-González et al., Monthly Notices of the Royal Astronomical Society **507**, 5144 (2021).

M. G. Aartsen, R. Abbasi, Y. Abdou et al., Physical Review Letters **111**, 10.1103/physrevlett.111.021103 (2013).

T. Bister and G. R. Farrar, The Astrophysical Journal **966**, 71 (2024).